

Light Stop in Precision Top Sample

Xue-Qian Li ^a, Zong-Guo Si ^b, Kai Wang ^c,

Liucheng Wang ^{c,d,*}, Liangliang Zhang ^{a,c}, and Guohuai Zhu ^c

^a *School of Physics, Nankai University, Tianjin 300071, China*

^b *Department of Physics, Shandong University, Jinan, Shandong 250100, China*

^c *Zhejiang Institute of Modern Physics, Department of Physics,
Zhejiang University, Hangzhou, Zhejiang 310027, China*

^d *Bartol Research Institute, Department of Physics and Astronomy,
University of Delaware, Newark, DE 19716, USA*

Abstract

The uncertainty of $t\bar{t}$ production cross section measurement at LHC is at a-few-percent level which still allows the stop pair production $t\bar{t}^*$ with identical visible final states $2b + \ell + nj + \cancel{E}_T$. In this paper, we attempt to use the existing measurement of W polarization in top quark decay to improve the distinction between stop and top quark states. We apply the ATLAS method of W -polarization measurement in semi-leptonic $t\bar{t}$ final state to semi-leptonic stop pair samples and study its prediction. We find that the faked top events from stop mostly contribute to the left-handed polarized W due to reconstruction and may enhance the F_L . The benchmark point with maximal contribution to top events only changes F_L by 1%. After comparing with the current experiments, we conclude that the current measurement of W -polarization in t decay cannot exclude the light stop scenario with stop mass around top quark mass.

*Electronic address: lcwang@udel.edu; (Corresponding Author)

I. INTRODUCTION

The Higgs boson has been discovered by both ATLAS and CMS Collaborations at the Large Hadron Collider (LHC). The data on the angular correlation in four-lepton channel prefers the boson to be identified as a CP-even spin zero $J = 0^+$ state [1]. The over- 5σ evidence in the four-lepton channel shows that the boson has a significant coupling to ZZ [1] and is indeed the Higgs boson which is responsible for electroweak symmetry breaking (EWSB). The combined analysis in the diphoton and four-lepton channels determines the reconstructed mass to be around 125 GeV [2].

If the Higgs boson is the fundamental scalar, quadratic divergence of the quantum correction to its mass is a major concern from the theoretical perspective. The low energy supersymmetry (SUSY) provides an elegant solution to this problem. Therefore it is generally believed that the SUSY theory should be a natural extension of the Standard Model (SM). But so far, the direct search for SUSY particles is not successful, one may wonder if the SUSY particles really exist, but hide themselves in some processes or have been misidentified. In fact, exploring low energy supersymmetric effects is also one of the leading tasks at the LHC. With the data of 30 fb^{-1} integrated luminosity, LHC has pushed the limit for the new physics models, in particular, the models which predict new strongly interacting particles due to their large production rate. Squarks and gluino of the low energy supersymmetric model suffer from severe constraints of direct searches at LHC through various processes, for instance, jets plus missing transverse energy $nj + \cancel{E}_T$ or jets plus \cancel{E}_T with leptons and etc. In some models the first two generation squark and gluino masses have been pushed as [3]

$$M_{\tilde{g}} > 1.4 \text{ TeV}, M_{\tilde{q}} > 1 \text{ TeV} . \quad (1)$$

For the third generation squark, assuming $\text{Br}(\tilde{t}_1 \rightarrow t + \tilde{\chi}_1^0) = 100\%$, the stop mass between 200 and 610 GeV has been excluded at 95% confidence level for massless $\tilde{\chi}_1^0$, and the stop mass around 500 GeV is excluded for $\tilde{\chi}_1^0$ masses up to 250 GeV [4]. If the mass difference between stop and top quark is less than or comparable with $\tilde{\chi}_1^0$, such a scenario has not yet been excluded by experimental data. Stop in such a mass range dominantly decays into bottom quark and the lightest chargino $\tilde{\chi}_1^\pm$. Thus a stop pair production may be misidentified as a SM $t\bar{t}$ event. The exclusion limit on the stop mass depends on an assumptions about the mass hierarchy of stop, $\tilde{\chi}_1^\pm$ and $\tilde{\chi}_1^0$ [4, 5].

Actually, due to enormous background from strong interacting quark-gluon scattering at this

proton-proton collider, only final state with certain distinguishable features can be triggered. Typical trigger requires the final states combined with hard jet possessing a transverse momentum $p_T^J > 120$ GeV, isolated leptons (e^\pm, μ^\pm) or photon (γ) passing basic cuts, large missing transverse energy (\cancel{E}_T) or object with secondary vertex (b -tag). A good example is the leptonic decay of a top quark which consists of a b -tagged jet, isolated e^\pm or μ^\pm and \cancel{E}_T . The trigger requirement also implies that the scenarios with a compressed spectrum are less constrained. Final states with hard jets and large missing transverse energy correspond to large mass difference in strongly interacting resonance with certain kinematics. Due to limited phase space in the compressed spectrum, the multi-body final state decays are typically suppressed while the loop-induced two-body decays often dominate in such cases, for instance, $\tilde{g} \rightarrow g\tilde{\chi}_1^0$ in gluino-bino co-annihilation scenario and $\tilde{t}_1 \rightarrow c\tilde{\chi}_1^0$ in stop-bino co-annihilation scenario. These signals with soft jet final states can easily be buried under the tremendous jet background. Back-to-back kinematics for the pair production of such gluinos or stops also reduces the missing transverse energy in the final states. Such final states can only be constrained by requiring additional initial state radiation (ISR) or final state radiation (FSR) jet via mono-jet plus \cancel{E}_T search. Hard isolated leptons require large chargino-neutralino mass difference $\Delta M = M_{\tilde{\chi}_1^\pm} - M_{\tilde{\chi}_1^0}$. Although the masses of $M_{\tilde{\chi}_1^\pm}$ and $M_{\tilde{\chi}_2^0}$ have been pushed up to 315 GeV if they decay through gauge bosons to a massless $\tilde{\chi}_1^0$ via direct search of tri-lepton plus \cancel{E}_T , the latest bound indeed leaves a corner of $M_{\tilde{\chi}_1^\pm} \simeq 150$ GeV with $M_{\tilde{\chi}_1^0} \simeq 100$ GeV [6]¹. On such a mass assumption, a light stop with mass around 190 GeV decaying with 100% branching ratio (BR) to a bottom quark and a chargino survives existing tests [5]. The assumption on a light stop and decoupled other sfermions seems to be plausible, because the Yukawa coupling of stop is much larger than other Yukawa couplings, which may affect drastically the renormalization group equations for the squark masses even if soft masses are the same at some high energy scale. For light stops, it is difficult to distinguish the events involving them from the enormous top-quark background. At LHC with the central energy 8 TeV, the $t\bar{t}$ production is

$$\sigma_{t\bar{t}}^{\sqrt{s}=8 \text{ TeV}} = 241 \pm 2(\text{stat.}) \pm 31(\text{syst.}) \pm 9(\text{lumi.}) \text{ pb}, \quad (2)$$

which is consistent with the theoretical prediction $\sigma_{t\bar{t}}^{\text{th}} = 238_{-24}^{+22}$ pb. For 200 GeV stop, its pair production is only 6 pb at LHC with the central energy 8 TeV. Even for 180 GeV stop, its pair

¹ Search of charginos from squark or gluino cascade decay in jets with lepton $nj + \cancel{E}_T + \ell^\pm$ puts stronger bounds on chargino masses but it's also model-dependent so we didn't take it account. Instead, we only take the direct search bounds which is more independent of model assumptions.

production is around 20 pb, which is still within the error bar of $t\bar{t}$ events.

On the other hand, the prompt decay of top quark before hadronization provides an opportunity to explore its various properties like charge and mass. This feature also makes the precision measurement of top quark possible. As a consequence of its huge mass $m_t = 173.2$ GeV, precision measurement of top quark plays an important role in testing the SM dynamics, for instance, the studies on the top-quark forward-backward asymmetry at Tevatron [7–10]. The precision measurement of weak decay of top quark is also a test of the Higgs mechanism. Both top quark and weak gauge boson W^\pm acquire masses from spontaneously EWSB. In so-called Higgs mechanism, the Goldstone degree of freedom becomes the longitudinal polarization of W boson, ϵ^0 . Since top quark is the heaviest particle from EWSB, top quark couples to the Goldstone boson more strongly which results in a m_t/m_W enhancement as $\epsilon_\mu^{0*} \bar{u}_b P_L \gamma^\mu u_t \propto m_t/m_W$. The W bosons from top-quark decay can be produced either longitudinal, left-handed or right-handed, with the helicity fractions F_0 , F_L and F_R respectively. Due to the m_t/m_W enhancement, one has $F_0 = \frac{(m_t/m_W)^2}{(m_t/m_W)^2+2} \simeq 70\%$, $F_L = \frac{2}{(m_t/m_W)^2+2} \simeq 30\%$ and $F_R = 0$ in the limit $m_b = 0$. Theoretically, the precision predictions of helicity fractions are obtained by next-to-next-to-leading order (NNLO) perturbative QCD (pQCD) calculations.

Because of the angular momentum conservation and neutrino being only left-handed, the helicity fractions F_0 , F_L and F_R can be measured by detecting the moving direction of the lepton from W -boson decay [11–15]. Experimentally, such precision measurements of helicity fractions require a full reconstruction of W boson and top quark. Thus only $t\bar{t}$ events with semileptonic decays are taken into account. The precision measurement of F_0 , F_L and F_R can test the V–A structure of the Wtb vertex, the Higgs mechanism as well as the NNLO pQCD calculation. If events of light stop pairs exist, they can also contribute to those measurements, since they can fake the semileptonic $t\bar{t}$ events. In this paper, we study whether the precision measurement of W -polarization in top sample can help to distinguish the light stop events, if they do exist, from the SM $t\bar{t}$ background.

In our studies, we employ the basic cuts described in [13]. We require the final states of semileptonic $t\bar{t}$ events to contain an isolated lepton (electron or muon), missing transverse momentum \cancel{E}_T and four jets with following p_T requirements:

- $p_T > 20$ GeV for an isolated electron or muon;
- $p_T > 25$ GeV and $|\eta| < 2.5$ for every jet.

Stop pair events and $t\bar{t}$ pairs have very different kinematic features and the events probabilities that pass the selection cuts are also different. Here, we use the survival probability after cuts ϵ to quantize the bounds. The cut survival probability depends on various factors, for instance, mass difference and polarization of gauginos. The p_T of b -jet or lepton significantly depends on the mass differences $M_{\tilde{t}} - M_{\chi_1^\pm}$ or $M_{\chi_1^\pm} - M_{\chi_1^0}$. Whether lepton is boosted or anti-boosted in the χ_1^\pm rest frame then depends on the polarization of χ_1^\pm which is determined by the mixing of wino and higgsino as well as the b -Yukawa coupling. However, if the chargino is produced nearly at rest, which is the case for the scenario we are focusing on, the boost or anti-boost effect of lepton is minor. In Table I, we list survival probabilities of a few benchmark points ². We also simulate the

	$M_{\tilde{t}}$ (GeV)	$M_{\chi_1^\pm}$ (GeV)	$M_{\chi_1^0}$ (GeV)	$\sigma_{t\bar{t}^*} \cdot \text{BR}$ (pb)	ϵ	$\epsilon \cdot \sigma_{t\bar{t}^*} \cdot \text{BR} \cdot K$ (pb)
A	150	110	80	8.205	0.06%	0.082
B	160	115	85	5.758	0.82%	0.08
C	170	130	90	4.222	1.35%	0.097
D	180	130	90	3.067	1.76%	0.092
E	190	140	95	2.27	2.49%	0.096
F	200	150	100	1.742	3.13%	0.0927

TABLE I: Survival probabilities after cuts for stop events and cross sections are shown for LHC@8TeV. NLO QCD K -factor is taken to be 1.7.

survival probability for semi-leptonic $t\bar{t}$ in SM at 8 TeV LHC.

$$\epsilon_{t\bar{t}}^{\text{SM}} = 14.42\% \quad (3)$$

The benchmark point C with maximal final rate in Table I only corresponds to the effective $t\bar{t}$ cross section as

$$0.097/\epsilon_{t\bar{t}}^{\text{SM}}/\text{BR} = 2.33 \text{ pb}, \quad (4)$$

which is within the uncertainty of cross section measurement.

This paper is organized as follow. In Section II, we discuss in detail how to measure W -polarization in the semi-leptonic $t\bar{t}$ events. Section III is devoted to the light stop scenario with

² We assume the sleptons are much heavier than chargino to minimize the flavor violation. Therefore, the chargino decay branching fraction is similar to the BR of the W boson.

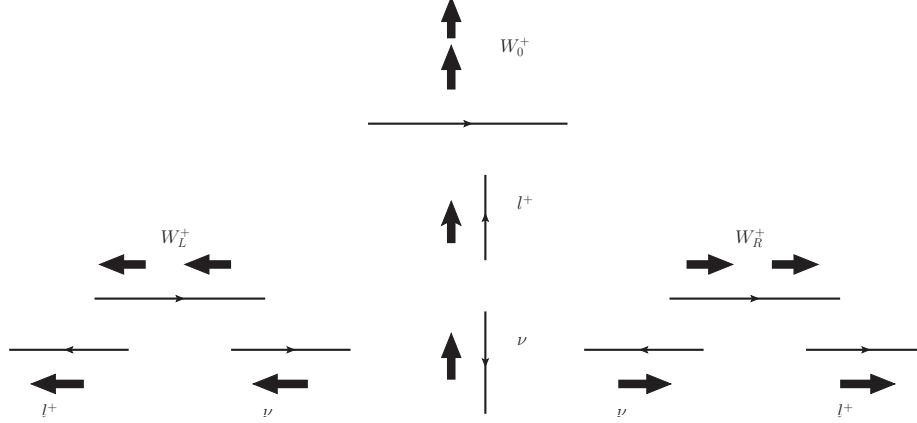


FIG. 1: The spin correlations between lepton l^+ and W -boson are shown for the left-handed polarized W_L^+ (left), the longitudinal polarized W_0^+ (center) and the right-handed polarized W_R^+ (right).

Higgs mass 125GeV. We show our results and analysis in Section IV and finally conclude with a summary in section V.

II. MEASUREMENTS OF W POLARIZATION IN THE SEMILEPTONIC $t\bar{t}$ EVENTS

The W boson from top-quark decay can be produced either longitudinal, left-handed or right-handed, with the helicity fractions F_0 , F_L and F_R respectively. The sum of the helicity fractions satisfies $F_L + F_R + F_0 = 1$. Measurements of these helicity fractions are very important to test the V - A structure of the SM, the Higgs mechanism, and the NNLO pQCD calculation. Experimentally, helicity fractions are firstly measured by the CDF and D0 experiments at Fermilab [11]. In the early 7 TeV-8 TeV running of the LHC, precision studies of W -boson polarization from top-quark decay have also been performed by both the ATLAS and CMS Collaborations [12–15]. All experiments require to detect the moving direction of the lepton from W -boson decay [16]. For the ATLAS Collaboration, they define the angle θ^* between the momentum direction of the lepton from the W -boson decay and the reversed momentum direction of the bottom quark from top-quark decay, both boosted into the W -boson rest frame [12–14]. For the CMS Collaboration, they use an equivalent definition as the angle θ^* between the three momentum of charged lepton in the W rest frame and the W momentum in the top rest frame [15]. Because the W boson must be fully reconstructed for each event, only semi-leptonic $t\bar{t}$ final state can be taken into account. The spin correlations of the process $W^+ \rightarrow l^+ \nu$ are shown in Fig. (1) for different polarized W -boson. Because of the angular momentum conservation and neutrino being only left-handed,

the lepton l^+ is boosted in the opposite moving direction of left-handed polarized W_L^+ . Namely, $\mathcal{M}(W_L^+ \rightarrow l^+\nu) \propto (1 - \cos \theta^*)^2$. By that analogy, l^+ is boosted in the same moving direction of right-handed polarized W_R^+ with $\mathcal{M}(W_R^+ \rightarrow l^+\nu) \propto (1 + \cos \theta^*)^2$. For the longitudinal polarized W_0^+ , the lepton l^+ is generally moving in the vertical direction with $\mathcal{M}(W_0^+ \rightarrow l^+\nu) \propto \sin^2 \theta^*$. The normalized decay rate of the process $t \rightarrow W^+b$, $W^+ \rightarrow l^+\nu$ can be given as

$$\frac{1}{\Gamma} \frac{d\Gamma}{d \cos \theta^*} = \frac{3}{8}(1 - \cos \theta^*)^2 F_L + \frac{3}{8}(1 + \cos \theta^*)^2 F_R + \frac{3}{4} \sin^2 \theta^* F_0. \quad (5)$$

In SM, the $V-A$ structure of the Wtb vertex contributes to the left-handed helicity fraction. The longitudinal helicity comes from the Goldstone boson component of W boson after EWSB while the right-handed helicity fraction is suppressed by the mass of bottom-quark m_b . In the limit $m_b = 0$ as the leading order, F_R is vanishing with $F_L = \frac{2}{(m_t/m_W)^2+2}$ and $F_0 = \frac{(m_t/m_W)^2}{(m_t/m_W)^2+2}$. So the helicity fractions are approximately 30% left-handed and 70% longitudinal. Including the finite bottom-quark mass and electroweak effects, NNLO pQCD predictions for the W-boson helicity fractions are $F_L = 0.311$, $F_R = 0.0017$ and $F_0 = 0.687$ [17].

In order to obtain the distribution of $\cos \theta^*$, we need to reconstruct W boson and top quark in each semi-leptonic $t\bar{t}$ event. Four-momentum information of lepton or jet final state is experimentally available. For the neutrino final state, its p_x and p_y component can be fixed by the measured missing transverse momentum in each semi-leptonic $t\bar{t}$ event. For the p_z component of neutrino, we fix it by using the χ^2 method given by the ATLAS Collaboration [13]. Here the χ^2 is defined as

$$\chi^2 = \frac{(m_{l\nu j_a} - m_t)^2}{\sigma_t^2} + \frac{(m_{j_b j_c j_d} - m_t)^2}{\sigma_t^2} + \frac{(m_{l\nu} - m_W)^2}{\sigma_W^2} + \frac{(m_{j_c j_d} - m_W)^2}{\sigma_W^2}, \quad (6)$$

with the top-quark mass $m_t = 172.5$ GeV, the W -boson mass $m_W = 80.4$ GeV, the expected top-quark mass resolution $\sigma_t = 14$ GeV and the expected W -boson mass resolution $\sigma_W = 10$ GeV. Here l denotes the isolated lepton and ν denotes the neutrino. $j_{a,b,c,d}$ are four different jets in each event. In this paper, we don't use any b-tagging information of each jet. $m_{l\nu j_a}$ is the invariant mass of the lepton l , the neutrino ν and the jet j_a . By that analogy, $m_{j_b j_c j_d}$, $m_{l\nu}$ and $m_{j_c j_d}$ are all invariant masses. For each semi-leptonic $t\bar{t}$ event, we scan the p_z of neutrino from -3.5 TeV to 3.5 TeV and make $j_{a,b,c,d}$ correspond to all possible combinations of four jets. By minimizing the χ^2 , we obtain the correct p_z component of neutrino [13]. Moreover, we can distinguish one b-jet, which accompanies with a leptonic W -boson, from other jets. So each semi-leptonic $t\bar{t}$ event can be fully reconstructed via this best pairing. No event is rejected according to this χ^2 method. $\cos \theta^*$ can be analyzed event by event.

Then the exact values of F_L , F_R and F_0 are determined with angular asymmetries. By counting events, one can always define an angular asymmetry as

$$A_Z = \frac{N(\cos \theta^* > z) - N(\cos \theta^* < z)}{N(\cos \theta^* > z) + N(\cos \theta^* < z)} \quad (7)$$

with $-1 \leq z \leq 1$. The most obvious choice is $z = 0$, which leads to the well-known forward-backward (FB) asymmetry A_{FB} . When we integrate $\cos \theta^*$ out in Eq. (5), A_{FB} depends only on F_L and F_R as $A_{\text{FB}} = \frac{3}{4}(F_R - F_L)$. Two additional choices of angular asymmetries can be conveniently defined by choosing $z_+ = -(2^{2/3} - 1)$ and $z_- = 2^{2/3} - 1$. Integrated $\cos \theta^*$ out in Eq. (5), one has $A_+ = 3\beta[F_0 + (1 + \beta)F_R]$ and $A_- = -3\beta[F_0 + (1 + \beta)F_L]$ with $\beta = 2^{1/3} - 1$. Using A_{FB} , A_+ and A_- as input under the constraint $F_L + F_R + F_0 = 1$, the helicity fractions of W -boson from top-quark decay can be obtained as

$$\begin{cases} F_L = \frac{1}{1-\beta} - \frac{A_+ - \beta A_-}{3\beta(1-\beta^2)}, \\ F_R = \frac{1}{1-\beta} + \frac{A_- - \beta A_+}{3\beta(1-\beta^2)}, \\ F_0 = -\frac{1+\beta}{1-\beta} + \frac{A_+ - A_-}{3\beta(1-\beta)}. \end{cases} \quad (8)$$

III. LIGHT STOP AND 125 GEV HIGGS BOSON

In the decoupling MSSM limit, the 125 GeV new particle can be identified as the lightest CP-even Higgs boson h . At tree level, the Higgs mass of h is determined as $m_h^2 = m_Z^2 \cos^2 2\beta$. The dominating loop contribution comes from the top/stop sector. If the splitting of the stop masses is relatively small, the mass of h up to 1-loop precision is [18]

$$m_h^2 \simeq m_Z^2 \cos^2 2\beta + \frac{3m_t^4}{4\pi^2 v^2} \left[\log \frac{M_{\text{SUSY}}^2}{m_t^2} + \frac{\tilde{A}_t^2}{M_{\text{SUSY}}^2} \left(1 - \frac{\tilde{A}_t^2}{12M_{\text{SUSY}}^2} \right) \right], \quad (9)$$

with EWSB vacuum expectation values (VEV) $v = 174$ GeV, the averaged stop mass square $M_{\text{SUSY}}^2 = m_{\tilde{t}_1} m_{\tilde{t}_2}$. Here $\tilde{A}_t = A_t - \mu \cot \beta$ with $\tan \beta$ the ratio of the VEVs of the two Higgs fields which lead to EWSB, A_t the trilinear squark coupling which breaks the R -symmetry, and μ Higgsino mass parameter, respectively. The term $\frac{\tilde{A}_t^2}{M_{\text{SUSY}}^2} \left(1 - \frac{\tilde{A}_t^2}{12M_{\text{SUSY}}^2} \right)$ reaches its maximum when $\tilde{A}_t^2/M_{\text{SUSY}}^2 = 6$, which corresponds to the maximal Higgs mass scenario. In order to predict $m_h=125$ GeV in the MSSM, a large \tilde{A}_t is necessary for moderate light stops [19–27]. In the meantime, the stop mass matrix is

$$\mathcal{M}_{\tilde{t}}^2 = \begin{pmatrix} m_{\tilde{t}_L}^2 + m_t^2 + D_L^t & m_t \tilde{A}_t \\ m_t \tilde{A}_t & m_{\tilde{t}_R}^2 + m_t^2 + D_R^t \end{pmatrix}. \quad (10)$$

Here $m_{\tilde{t}_L}$ and $m_{\tilde{t}_R}$ are the left-handed and right-handed soft SUSY breaking stop masses. The D terms, in units of $M_Z^2 \cos 2\beta$, are given in terms of the weak isospin and electric charge of the stop by: $D_L^t = I_t^3 - e_t \sin^2 \theta_W$ and $D_R^t = e_t \sin^2 \theta_W$. This stop mass matrix can be diagonalized by a unitary matrix to give mass eigenstates \tilde{t}_1 and \tilde{t}_2 . For moderate $m_{\tilde{t}_L}$ and $m_{\tilde{t}_R}$, \tilde{A}_t ought to be large to predict $m_h=125$ GeV. Such a large off-diagonal term $m_t \tilde{A}_t$ would lead to a big splitting of stop masses. So the scenario with a light \tilde{t}_1 is possible and \tilde{t}_1 should be around 50% of \tilde{t}_L and 50% of \tilde{t}_R . These features are maintained in NMSSM with a small λ but changed in NMSSM with a large λ . This is because $m_h^2 = m_Z^2 \cos^2 2\beta + \lambda^2 v^2 \sin 2\beta$ at tree-level in NMSSM. Here the second term $\lambda^2 v^2 \sin 2\beta$ originates from the interaction $\lambda H_u H_d S$ in the superpotential, where S is the singlet in NMSSM. Due to the extra contribution $\lambda^2 v^2 \sin 2\beta$ to Higgs mass at tree level, it would be easier to realize a 125 GeV Higgs boson in NMSSM [28, 29]. A large \tilde{A}_t may not be necessary. The light mass eigenstate \tilde{t}_1 may be pure \tilde{t}_L or pure \tilde{t}_R in NMSSM.

As argued in the previous section, the scenario with $m_{\tilde{t}_1} = 200$ GeV, $\tilde{\chi}_1^\pm = 150$ GeV and $\tilde{\chi}_1^0 = 100$ GeV has not yet been excluded by existing experimental data. In this case, \tilde{t}_1 decays totally into bottom-quark and chargino. The polarization of chargino from stop decay has been recently discussed in [30]. In the MSSM, the relevant Lagrangians involving $\tilde{t}_1 \rightarrow b \tilde{\chi}_1^+$ are following [31]

$$\mathcal{L}_{b\tilde{t}_1\tilde{\chi}_1^+} = \{[-gV_{11}\tilde{t}_L + y_t V_{12}\tilde{t}_R]\bar{b}P_R + y_b U_{12}\tilde{t}_L\bar{b}P_L\}\tilde{\chi}_1^{+c}. \quad (11)$$

Here U_{ij} (V_{ij}) are the neutralino (chargino) mixing matrices and y_t (y_b) is the top (bottom) Yukawa coupling. The mass eigenstate $\tilde{\chi}_1^+$ is combined by wino and higgsino, which is determined by the wino parameter M_2 and the higgsino parameter μ . In Eq. (11), the wino component of $\tilde{\chi}_1^+$ contributes to the first term while the higgsino component contributes to two other terms. In the rest frame of stop, $\tilde{\chi}_1^+$ and the bottom-quark are produced back to back. If the chargino is pure wino-like, the \tilde{t}_L component of \tilde{t}_1 decays into $\tilde{\chi}_1^+$ via the first term of Eq. (11). In this case $\tilde{\chi}_1^+$ is always in the left-handed helicity eigenstate since this wino-stop-bottom vertex is corresponding to the weak interaction. Left-hand $\tilde{\chi}_1^+$ means that the spin is opposite to the direction of its motion. If chargino has a significant higgsino component, the \tilde{t}_R component of \tilde{t}_1 may decay into left-handed $\tilde{\chi}_1^+$ via the second term of Eq. (11). $\tilde{\chi}_1^+$ from stop decay can be right-handed via the third term of Eq. (11), which can be significantly enhanced by a large bottom Yukawa coupling y_b . Comparing to the top Yukawa coupling y_t , y_b can be significantly enhanced by a large $\tan \beta$ as

$$\frac{y_b}{y_t} = \frac{m_b}{\sqrt{2}v_d} / \frac{m_t}{\sqrt{2}v_u} = \frac{m_b}{m_t} \tan \beta$$

Similar to the process $t \rightarrow W^+ b$, $W^+ \rightarrow l^+ \nu$, there exists some spin correlation between lepton

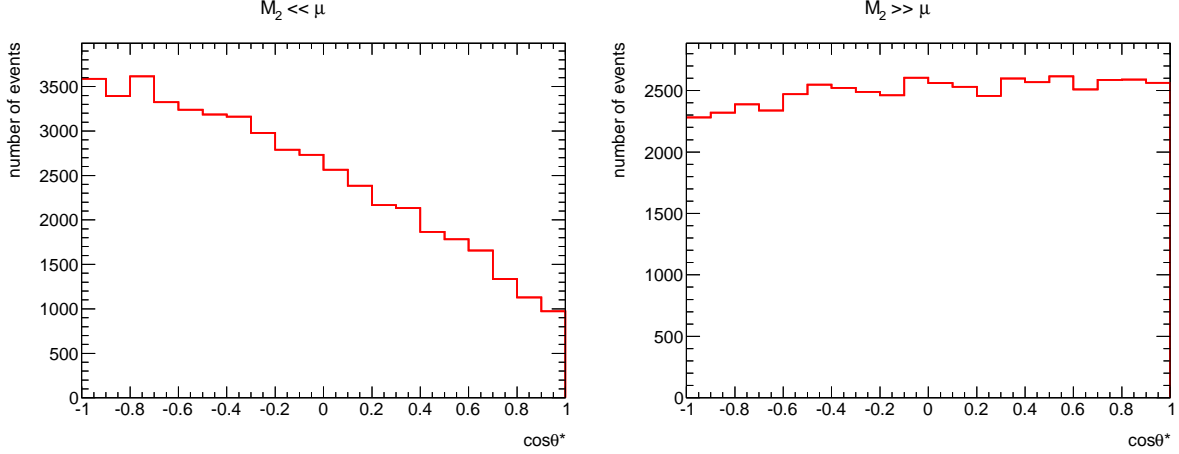


FIG. 2: At parton level, the chargino $\tilde{\chi}_1^+$ can be fully reconstructed since all information of neutralino, lepton and neutrino is known. We show the $\cos \theta^*$ distribution in the $\tilde{\chi}_1^+$ rest frame. Left: Assuming $M_2 \ll \mu$, the chargino is wino-like. The $\cos \theta^*$ distribution peaks at $\theta = \pi$ since the chargino from stop decay is mainly left-handed. Right: Assuming $\mu \ll M_2$ with a large $\tan \beta$, the chargino is higgsino-like as well as a large bottom Yukawa coupling y_b . So the right-handed helicity of the chargino is significant.

and chargino for the cascade decay $\tilde{t}_1 \rightarrow b\tilde{\chi}_1^+, \tilde{\chi}_1^+ \rightarrow \tilde{\chi}_1^0 l^+ \nu$. But for this case, the correlation is more complex due to chargino three-body decay mediated by slepton exchange and W-boson exchange. The angular distribution of the lepton from chargino decay can be used to partially probe the chargino polarization [32]. We can define the angle θ^* between the momentum direction of the lepton from chargino decay and the reversed momentum direction of bottom quark from stop decay, both boosted into the chargino rest frame. Because of angular momentum conservation, the distribution of $\cos \theta^*$ would in general peak at $\theta^* = \pi$ for left-handed $\tilde{\chi}_1^+$ [32]. If $\tilde{\chi}_1^+$ is totally in the right-handed helicity eigenstate, the distribution of $\cos \theta^*$ should peak at $\theta^* = 0$. To illustrate this feature, we consider two extreme cases in this paper. One is under the assumption $M_2 \ll \mu$, which leads to a nearly wino-like $\tilde{\chi}_1^+$. In this case $\tilde{\chi}_1^+$ from stop decay is always in the left-handed helicity. The other case bases on the assumption $M_2 \gg \mu$ as well as a large $\tan \beta$. So the right-handed helicity of the chargino is significant. In both cases, we assume $m_{\tilde{t}_1} = 200$ GeV, $\tilde{\chi}_1^\pm = 150$ GeV, $\tilde{\chi}_1^0 = 100$ GeV and all masses of sleptons around 1 TeV. We use the code Madgraph5 [33] to simulate the whole process. At parton level, the chargino can be fully reconstructed since all information of neutralino, lepton and neutrino is known. So the $\cos \theta^*$ distribution can be exactly obtained in the chargino rest frame at parton level. In Fig. (2), we show the $\cos \theta^*$ distribution

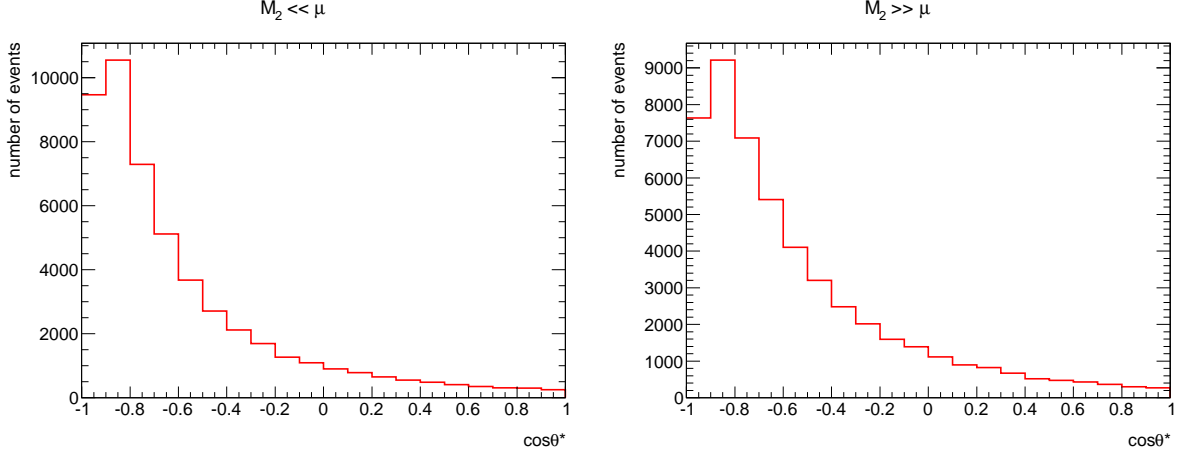


FIG. 3: Left: $M_2 \ll \mu$. Right: $\mu \ll M_2$ with a large $\tan \beta$. The $\cos \theta^*$ distribution of stop events are given in the fake W -boson rest frame after χ^2 combination. Both figures are shown at the parton level. The results after pythia and pgs will be similar to the parton level results.

under two different assumptions. We find that the right-handed helicity of $\tilde{\chi}_1^+$ can be significant if the lightest chargino is higgsino-like as well as a large $\tan \beta$. For W -boson from top-quark decay, the right-hand helicity fraction F_R is approximately vanishing and is severely constrained by experimental data. So in this paper, we would like to study whether such a right-hand helicity structure of $\tilde{\chi}_1^+$ from stop decay can help to distinguish the light stop events from the SM top-quark events.

IV. RESULTS AND ANALYSIS

Experimentally, we don't even know there exists chargino from stop decay. The final states from a semi-leptonic decay of $\tilde{t}_1 \tilde{t}_1^*$ are an isolated lepton, missing transverse energy \cancel{E}_T , two bottom-quark jets and two light-quark jets. With identical final states, $\tilde{t}_1 \tilde{t}_1^*$ events will be misidentified as the SM top events. So the $\cos \theta^*$ distribution in the $\tilde{\chi}_1^+$ rest frame, as shown in Fig. (2), cannot be experimentally measured. The ATLAS method of W -polarization measurement in semi-leptonic $t\bar{t}$ final state will be applied to semi-leptonic stop pair samples. We would like to study this prediction of $\tilde{t}_1 \tilde{t}_1^*$. Firstly, the ATLAS χ^2 method will lead to a fake p_Z component of neutrino momentum. For each $\tilde{t}_1 \tilde{t}_1^*$ event, the fake p_Z may be far from the real value since the lightest neutralino $\tilde{\chi}_1^0$ also contributes to missing transverse energy \cancel{E}_T . Secondly, the χ^2 method inevitably results in a fake W -boson rest frame for each $\tilde{t}_1 \tilde{t}_1^*$ event. The $\cos \theta^*$ distribution can only

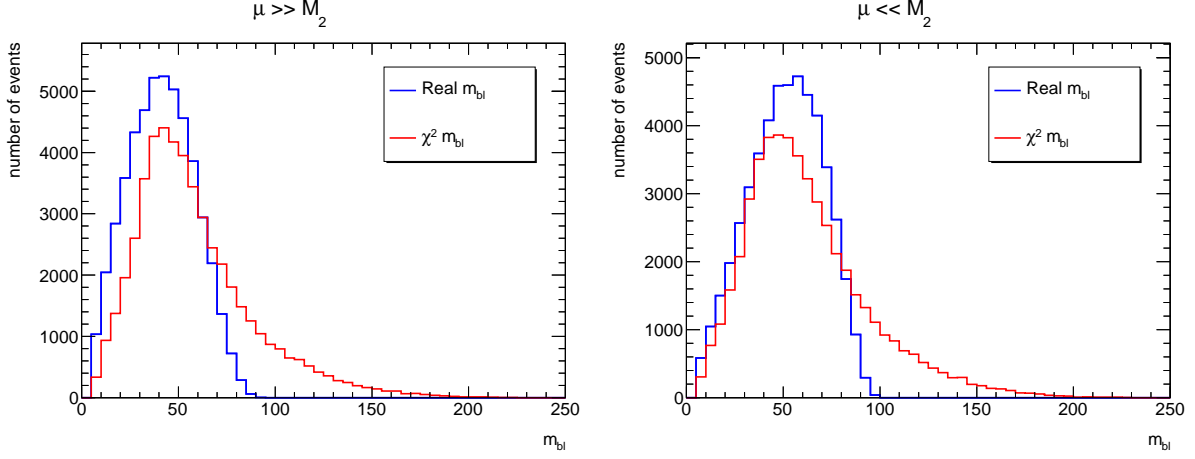


FIG. 4: Left: $M_2 \ll \mu$. Right: $\mu \ll M_2$ with a large $\tan \beta$. The blue line is M_{bl} in the real combination while the red line is M_{bl} after χ^2 combination. All results about stop events are shown at the parton level.

be obtained in such a fake W -boson rest frame. Lastly, for some $\tilde{t}_1 \tilde{t}_1^*$ events, a fake leptonic-branch b-jet may be picked out of the four jets by minimizing the χ^2 . If so, the reversed momentum direction of the bottom quark, which accompanies with a leptonic W boson, is incorrect. This wrong momentum also leads to a fake $\cos \theta^*$. In fig. (3), we show the $\cos \theta^*$ distribution of stop events in fake W -boson rest frame after χ^2 method. The left figure is corresponding to the assumption $M_2 \ll \mu$ while the right figure is corresponding to the assumption $\mu \ll M_2$ with a large $\tan \beta$. Both $\cos \theta^*$ distributions peak at $\theta^* = \pi$. These behaviors are generally corresponding to left-handed helicity states. Since the W boson from top-quark decay is roughly 30% left-handed, it seems to be hard to distinguish the light stop event from SM background by analyzing the polarization.

But we know that the right-handed helicity of the chargino from stop decay is significant under the assumption $\mu \ll M_2$ with a large $\tan \beta$, as shown in the right of fig. (2). In fig. (2), $\cos \theta^*$ is defined in the chargino rest frame in order to probe the polarization of chargino. Unfortunately, it cannot be experimentally measured. When the χ^2 method of W -polarization measurement in semi-leptonic $t\bar{t}$ final state is applied to semi-leptonic stop pair events, $\cos \theta^*$ can only be defined in the W -boson rest frame. In the right of fig. (3), the right-handed component seems disappeared. To understand the $\cos \theta^*$ distribution, we focus on a general definition of angle θ^* , which is between the momentum direction of the lepton and the reversed momentum direction of the bottom quark, both boosted into a specific chosen frame. Thus $\cos \theta^* = -\frac{\vec{p}_l \cdot \vec{p}_b}{|\vec{p}_l| |\vec{p}_b|}$, where the momentum \vec{p}_l and \vec{p}_b depend on the chosen frame. Since the lepton and bottom quark are approximately massless, we

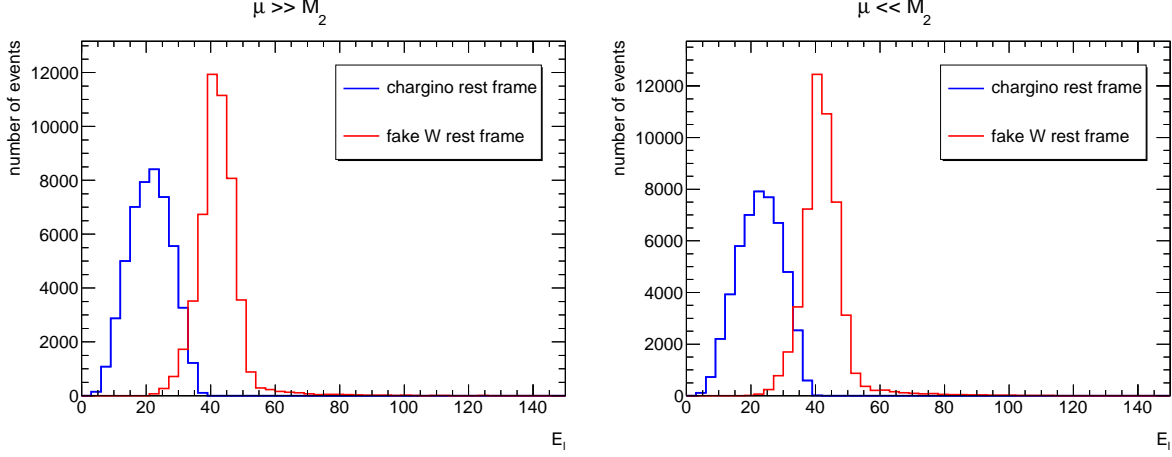


FIG. 5: Left: $M_2 \ll \mu$. Right: $\mu \ll M_2$ with a large $\tan \beta$. The blue line is E_l boosted into the real $\tilde{\chi}_1^+$ rest frame while the red line is E_l boosted into the fake W -boson rest frame after χ^2 combination.

rewrite $\cos \theta^*$ as

$$\begin{aligned} \cos \theta^* &= \frac{E_l \cdot E_b - \vec{p}_l \cdot \vec{p}_b - E_l \cdot E_b}{|\vec{p}_l| |\vec{p}_b|} = \frac{p_l \cdot p_b}{|\vec{p}_l| |\vec{p}_b|} - 1 \\ &= \frac{M_{lb}^2}{2E_l E_b} - 1. \end{aligned} \quad (12)$$

Here M_{lb} is the invariant mass of the lepton and bottom quark. E_l (E_b) is the energy of lepton (bottom quark), which depends on the chosen frame. For stop events in the chargino rest frame, $E_b = \frac{m_{\tilde{t}_1}^2 - m_{\tilde{\chi}_1^+}^2}{2m_{\tilde{\chi}_1^+}}$ is fixed due to energy-momentum conservation. In order to understand the fake polarization, we show M_{bl} , E_l and E_b of the stop events in Fig. (4), Fig. (5) and Fig. (6), respectively.

In Fig. (4), the blue line is M_{bl} in the real combination while the red line is M_{bl} after χ^2 combination. Since M_{bl} is Lorentz invariant, it is independent of the chosen frame. The difference between the real combination and χ^2 combination only originates from the wrong combination of lepton and bottom quark after minimizing the χ^2 . For some $\tilde{t}_1 \tilde{t}_1^*$ events, a fake leptonic-branch b-jet may be picked out of the four jets to get M_{bl} . Since we do not use the b-tagging information of four jets in our paper, even a light-quark jet might be faked as the leptonic-branch b-jet. To reduce the events with the wrong combination, we suggest to use b-tagging in the χ^2 reconstruction. However, from Fig. (4) we know that the distributions of real and fake M_{bl} of stop events are similar. In Fig. (5), we show the distribution of E_l from the light stop events. The blue line is E_l boosted into the real $\tilde{\chi}_1^+$ rest frame while the red line is E_l boosted in the fake W -boson rest

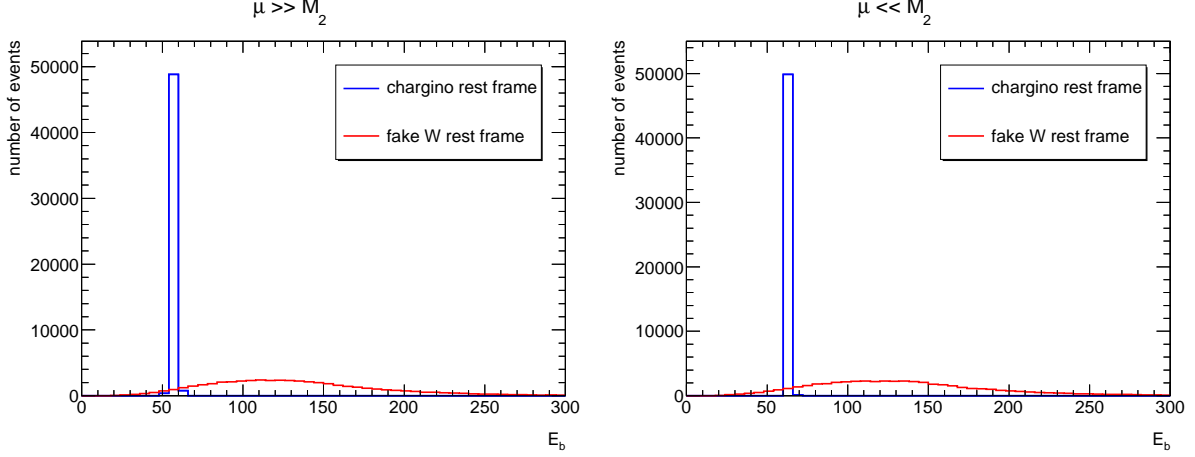


FIG. 6: Left: $M_2 \ll \mu$. Right: $\mu \ll M_2$ with a large $\tan \beta$. The blue line is E_b boosted into the real $\tilde{\chi}_1^+$ rest frame while the red line is E_b boosted into the fake W -boson rest frame after χ^2 combination.

frame after χ^2 combination. E_l in the fake W -boson rest frame are generally larger than one in the real $\tilde{\chi}_1^+$ rest frame. Moreover, E_l in the fake W -boson rest frame roughly peaks at 40 GeV. For $t\bar{t}$ events in the W -boson rest frame, we know that $E_l = \frac{M_W}{2} = 40$ GeV due to energy-momentum conservation. So after the χ^2 method is applied to semi-leptonic stop pair events, the distribution of E_l from stop decay becomes similar to E_l from top-quark decay. E_b are shown in Fig. (6). E_b in blue line is in the real $\tilde{\chi}_1^+$ rest frame and E_b in red line is in the fake W -boson rest frame after χ^2 combination. Because of energy-momentum conservation, E_b in the real $\tilde{\chi}_1^+$ rest frame is fixed to $E_b = \frac{m_{t_1}^2 - m_{\tilde{\chi}_1^+}^2}{2m_{\tilde{\chi}_1^+}} = \frac{200^2 - 150^2}{2 \times 150}$ GeV = 58 GeV. In general, we can see that E_b in the fake W -boson rest frame are larger than E_b in the real $\tilde{\chi}_1^+$ rest frame.

Finally, we show the combination $\sqrt{E_b E_l}$ of stop-pair events in Fig. (7). The blue line is corresponding to $\sqrt{E_b E_l}$ boosted into the real $\tilde{\chi}_1^+$ rest frame while the red line is corresponding to $\sqrt{E_b E_l}$ boosted into the fake W -boson rest frame after χ^2 combination. In both the left and the right figure, $\sqrt{E_b E_l}$ in the fake W -boson rest frame is larger than $\sqrt{E_b E_l}$ in the real $\tilde{\chi}_1^+$ rest frame. According to Eq. (12), this first term in the second line is suppressed by $E_b E_l$. So comparing to $\cos \theta^*$ in the real $\tilde{\chi}_1^+$ rest frame, $\cos \theta^*$ in the W -boson rest frame is consequently approaching to -1. That is why both of fake $\cos \theta^*$ distributions in Fig. (3) peak at $\theta^* = \pi$. Correspondingly, $\cos \theta^*$ distributions in the chargino rest frame, as shown in Fig. (2), are more even in the $\cos \theta^*$ range $[-1, 1]$.

In both the left and right figure of Fig. (7), one can see that the $\sqrt{E_b E_l}$ distribution of stop-pair

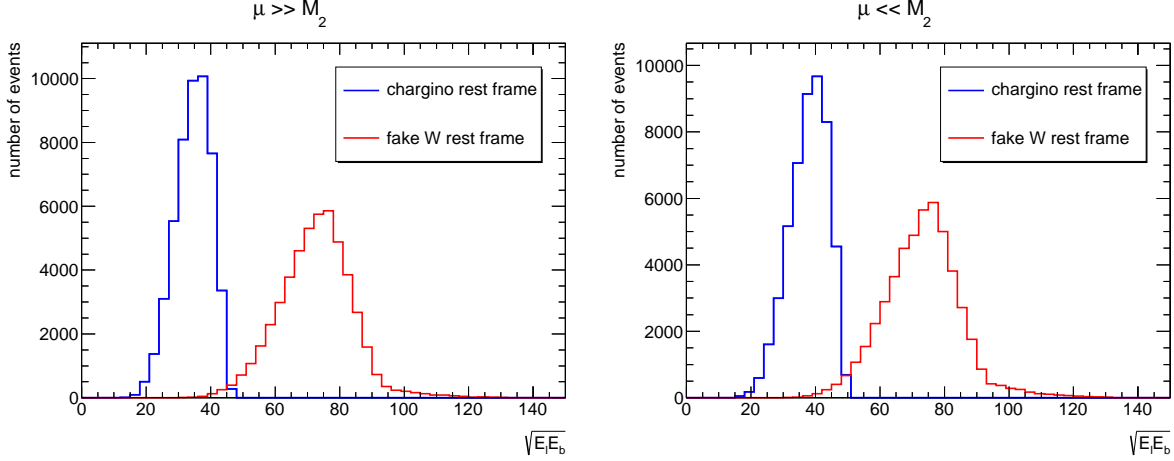


FIG. 7: Left: $M_2 \ll \mu$. Right: $\mu \ll M_2$ with a large $\tan \beta$. The blue line is $\sqrt{E_b E_l}$ boosted into the real $\tilde{\chi}_1^+$ rest frame while the red line is $\sqrt{E_b E_l}$ boosted into the fake W -boson rest frame after χ^2 combination.

events in the fake W -boson rest frame roughly peaks at $\sqrt{E_b E_l} = 75$ GeV. In the meanwhile, because of energy-momentum conservation, we know $E_b = \frac{m_t^2 - m_W^2}{2m_W}$ and $E_l = \frac{m_W}{2}$ for $t\bar{t}$ events in the W -boson rest frame. Thus for $t\bar{t}$ events in the W -boson rest frame, $\sqrt{E_b E_l} = \sqrt{\frac{m_t^2 - m_W^2}{4}} = 77$ GeV is fixed. So when the χ^2 method of semi-leptonic $t\bar{t}$ final state is applied to semi-leptonic stop-pair events, $\sqrt{E_b E_l}$ of stop-pair event in the fake W -boson rest frame is approximately similar to $\sqrt{E_b E_l}$ of top-quark event. That is, if the stop-pair event is reconstructed by the χ^2 method, the $\cos \theta^*$ distribution in the fake W -boson rest frame is approximately governed by the top-pair distribution as

$$\cos \theta^* = \frac{2M_{bl}^2}{m_t^2 - m_W^2} - 1. \quad (13)$$

Here the top-quark mass $m_t = 172.5$ GeV and the W -boson mass $m_W = 80.4$ GeV are defined in the χ^2 method, as shown in Eq. (6). When the χ^2 method of $t\bar{t}$ final states is applied to stop-pair events, m_t and m_W are not physical masses but expected masses. By minimizing the χ^2 , the final states of stop-pair events are expected to have resonances around the mass m_t and m_W . In order to prove Eq. (13), we would like to vary m_t in the χ^2 method. The first term of the right hand of Eq. (13) is suppressed by m_t^2 . If m_t becomes larger, the term $\frac{2M_{bl}^2}{m_t^2 - m_W^2}$ becomes small. More stop-pair events will fall into the $\cos \theta^*$ range near $\cos \theta^* = -1$. We vary m_t as 200 GeV, 400 GeV and 600 GeV in the χ^2 reconstruction and the results are shown in Fig. (8). As expected, the $\cos \theta^*$ distribution is approaching to -1 when m_t becomes larger. The $\cos \theta^*$ distribution of stop-pair events in the fake W -boson rest frame is proved to be governed by Eq. (13).

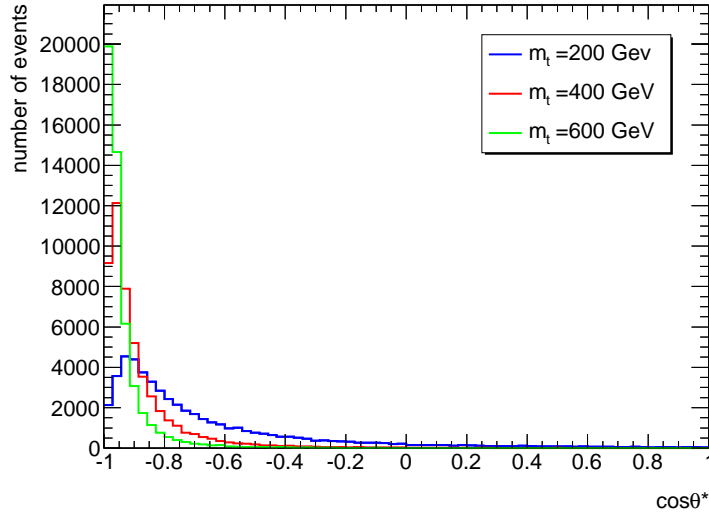


FIG. 8: The $\cos \theta^*$ distributions of stop-pair events are given in the W -boson rest frame when the top-quark mass m_t in the χ^2 method are varied.

V. CONCLUSION

The uncertainty of the $t\bar{t}$ production cross section at LHC is at a-few-percent level. This small range might accommodate new physics beyond SM, if taking it as a possible signal. The SUSY theory is generally believed to be a natural extension of the SM. So the gap can be attributed to a stop pair production $\tilde{t}\tilde{t}^*$ with identical final states $2b + \ell + nj + \cancel{E}_T$. Though low energy SUSY is suffering from severe constraints of direct searches at LHC, a light stop scenario with a compressed spectrum, such as $m_{\tilde{t}_1} = 200$ GeV, $\tilde{\chi}_1^\pm = 150$ GeV and $\tilde{\chi}_1^0 = 100$ GeV, has not yet been excluded. Stop in such a mass range will be mis-identified as a SM top-quark. In this paper, we attempt to use the precision measurement of W -polarization in top-quark decay to improve the ability to distinguish the light stop scenario from the SM top-quark background. The prompt decay of top-quark before hadronization makes the precision measurement of top-quark possible and such a measurement plays an important role in testing perturbative QCD as well as the Higgs mechanism. When the ATLAS χ^2 method of W -polarization measurement in semi-leptonic $t\bar{t}$ final state is applied to semi-leptonic stop-pair events, we find that the $\cos \theta^*$ distribution is always approaching to -1. The “faked” top events from stop mostly contribute to the left-handed polarized W -boson due to the “faked” full reconstruction of W -boson and top-quark. Since the W -boson from top-quark decay is roughly 30% left-handed, it is hard to distinguish the light stop event from

SM top background by analyzing the polarization. We compute the $F_L/F_R/F_0$ contribution from benchmark point C in Table. I, which is of the maximal contribution to $t\bar{t}$ events. After using Eq. (7) and Eq. (8), the result is listed as following:

$$\begin{aligned} \text{SM} : F_L &= 0.303, F_R = 0.0493, F_0 = 0.647, \\ \text{SM with stop} : F_L &= 0.313, F_R = 0.0497, F_0 = 0.638. \end{aligned} \tag{14}$$

The benchmark point with maximal contribution to top events only changes F_L by 1%, which is far below the current uncertainty. Thus, we conclude that the current measurement on the W -polarization cannot exclude the light stop scenario with stop mass around top-quark mass.

Acknowledgement

LW and LZ would like to thank Jiwei Ke for useful discussions about Madgraph5. XL is supported by the National Science Foundation of China (11075079, 11135009). ZS is supported by the National Science Foundation of China (11275114). KW is supported in part, by the Zhejiang University Fundamental Research Funds for the Central Universities (2011QNA3017) and the National Science Foundation of China (11245002, 11275168). GZ is supported in part, by the National Science Foundation of China (11075139, 11135006, 11375151) and the Program for New Century Excellent Talents in University (Grant No. NCET-12-0480).

-
- [1] Measurements of the properties of the higgs-like boson in the four lepton decay channel with the atlas detector using 25 fb^{-1} of proton-proton collision data. Technical Report ATLAS-CONF-2013-013.
 - [2] Combined measurements of the mass and signal strength of the Higgs-like boson with the ATLAS detector using up to 25 fb^{-1} of proton-proton collision data. Technical Report ATLAS-CONF-2013-014.
 - [3] Jared A. Evans, Yevgeny Kats, David Shih, and Matthew J. Strassler. Toward Full LHC Coverage of Natural Supersymmetry. 2013.
 - [4] Search for direct top squark pair production in final states with one isolated lepton, jets, and missing transverse momentum in $\sqrt{s} = 8, \text{TeV}$ pp collisions using 21 fb^{-1} of atlas data. Technical Report ATLAS-CONF-2013-037.

- [5] Search for direct top squark pair production in final states with two leptons in $\sqrt{s} = 8$ tev pp collisions using 20 fb^{-1} of atlas data. Technical Report ATLAS-CONF-2013-048.
- [6] Search for direct production of charginos and neutralinos in events with three leptons and missing transverse momentum in 21 fb^{-1} of pp collisions at $\sqrt{s} = 8$ tev with the atlas detector. Technical Report ATLAS-CONF-2013-035.
- [7] Measurement of the Forward Backward Asymmetry in Top Pair Production in the Dilepton Decay Channel using 5.1 fb^{-1} . Technical Report CDF Note 10436.
- [8] J.A. Aguilar-Saavedra, W. Bernreuther, and Z.G. Si. Collider-independent top quark forward-backward asymmetries: standard model predictions. *Phys.Rev.*, D86:115020, 2012.
- [9] Jun Gao, Chong Sheng Li, and Hua Xing Zhu. Top Quark Decay at Next-to-Next-to Leading Order in QCD. *Phys.Rev.Lett.*, 110:042001, 2013.
- [10] Jing Shu, Kai Wang, and Guohuai Zhu. A Revisit to Top Quark Forward-Backward Asymmetry. *Phys.Rev.*, D85:034008, 2012.
- [11] T. Aaltonen et al. Combination of CDF and D0 measurements of the W boson helicity in top quark decays. *Phys.Rev.*, D85:071106, 2012.
- [12] Georges Aad et al. Measurement of the W boson polarization in top quark decays with the ATLAS detector. *JHEP*, 1206:088, 2012.
- [13] Measurement of the W -boson polarisation in top quark decays in pp collision data at $\sqrt{s} = 7$ TeV using the ATLAS detector. Technical Report ATLAS-CONF-2011-037.
- [14] Combination of the ATLAS and CMS measurements of the W -boson polarization in top-quark decays. Technical Report ATLAS-CONF-2013-033.
- [15] Measurement of the W boson polarization in semileptonic top pair decays with the CMS detector at the LHC. Technical Report CMS-PAS-TOP-11-020.
- [16] Gordon L. Kane, G.A. Ladinsky, and C.P. Yuan. Using the Top Quark for Testing Standard Model Polarization and CP Predictions. *Phys.Rev.*, D45:124–141, 1992.
- [17] Andrzej Czarnecki, Jurgen G. Korner, and Jan H. Piclum. Helicity fractions of W bosons from top quark decays at NNLO in QCD. *Phys.Rev.*, D81:111503, 2010.
- [18] Marcela S. Carena, J.R. Espinosa, M. Quiros, and C.E.M. Wagner. Analytical expressions for radiatively corrected Higgs masses and couplings in the MSSM. *Phys.Lett.*, B355:209–221, 1995.
- [19] Lawrence J. Hall, David Pinner, and Joshua T. Ruderman. A Natural SUSY Higgs Near 126 GeV. *JHEP*, 1204:131, 2012.

- [20] Patrick Draper, Patrick Meade, Matthew Reece, and David Shih. Implications of a 125 GeV Higgs for the MSSM and Low-Scale SUSY Breaking. *Phys.Rev.*, D85:095007, 2012.
- [21] Marcela Carena, Stefania Gori, Nausheen R. Shah, and Carlos E.M. Wagner. A 125 GeV SM-like Higgs in the MSSM and the $\gamma\gamma$ rate. *JHEP*, 1203:014, 2012.
- [22] A. Arbey, M. Battaglia, A. Djouadi, F. Mahmoudi, and J. Quevillon. Implications of a 125 GeV Higgs for supersymmetric models. *Phys.Lett.*, B708:162–169, 2012.
- [23] S. Heinemeyer, O. Stal, and G. Weiglein. Interpreting the LHC Higgs Search Results in the MSSM. *Phys.Lett.*, B710:201–206, 2012.
- [24] Jiwei Ke, Ming-Xing Luo, Lian-You Shan, Kai Wang, and Liucheng Wang. Searching SUSY Leptonic Partner at the CERN LHC. *Phys.Lett.*, B718:1334–1341, 2013.
- [25] Jiwei Ke, Hui Luo, Ming-xing Luo, Kai Wang, Liucheng Wang, et al. Revisit to Non-decoupling MSSM. *Phys.Lett.*, B723:113–119, 2013.
- [26] Jiwei Ke, Hui Luo, Ming-xing Luo, Tian-yang Shen, Kai Wang, et al. What if $b\bar{b}$ does not dominate the decay of the Higgs-like boson? 2012.
- [27] Tao Han, Tong Li, Shufang Su, and Lian-Tao Wang. Non-Decoupling MSSM Higgs Sector and Light Superpartners. *JHEP*, 1311:053, 2013.
- [28] Jun-Jie Cao, Zhao-Xia Heng, Jin Min Yang, Yan-Ming Zhang, and Jing-Ya Zhu. A SM-like Higgs near 125 GeV in low energy SUSY: a comparative study for MSSM and NMSSM. *JHEP*, 1203:086, 2012.
- [29] Junjie Cao, Fangfang Ding, Chengcheng Han, Jin Min Yang, and Jingya Zhu. A light Higgs scalar in the NMSSM confronted with the latest LHC Higgs data. *JHEP*, 1311:018, 2013.
- [30] Ian Low. Polarized Charginos (and Tops) in Stop Decays. 2013.
- [31] Howard E. Haber and Gordon L. Kane. The Search for Supersymmetry: Probing Physics Beyond the Standard Model. *Phys. Rept.*, 117:75–263, 1985.
- [32] Mingxing Luo, Xu Tao, Kai Wang, Liucheng Wang, and Guohuai Zhu. To appear.
- [33] Johan Alwall, Michel Herquet, Fabio Maltoni, Olivier Mattelaer, and Tim Stelzer. MadGraph 5 : Going Beyond. *JHEP*, 1106:128, 2011.